Structural and Electronic Characterization of m-Fluoroaniline and m-Iodoaniline: A Density Functional Theory Study

Yavuz EKİNCİOĞLU 1* and Abdullah KEPCEOĞLU 2,3

1 Bayburt University, Department of Opticianry, 69000, Bayburt, TÜRKİYE
2 Koç University, Department of Molecular Biology and Genetics, 34450, İstanbul, TÜRKİYE
3 Koç University Surface Science and Technology Center (KUYTAM), Rumelifeneri, Istanbul, 34450, Turkey

* Corresponding author e-mail address: yekincioglu@bayburt.edu.tr

ORCID Numbers: 0000-0002-8610-1245 (Yavuz EKİNCİOĞLU), 0000-0002-4743-5517 (Abdullah KEPCEOĞLU)

Abstract

This study aimed to investigate the electronic and structural characteristics of m-fluoroaniline (MFA) and m-iodoaniline (MIA). Density functional theory (DFT) and CAM-B3LYP/LanL2DZ methods were employed to determine various properties such as the highest occupied molecular orbital (HOMO) and lowest unoccupied molecular orbital (LUMO) energy levels, chemical reactivity descriptors, nonlinear optical properties, Mulliken population analysis, molecular electrostatic potential map, thermodynamic properties, and UV-Vis spectral analysis. In addition, the research explored the vertical and adiabatic ionization energy parameters of these molecules by constructing singly charged cation radicals using the same level theory. The obtained results were compared with experimental data from the literature.

Keywords — DFT, Molecular properties, HOMO, LUMO, NLO, UV-Vis, Adiabatic Ionization, Vertical Ionization

1. INTRODUCTION

Aromatic amines, especially aniline, are crucial in biology and materials science due to their numerous technological uses [1, 2]. Aniline serves as a precursor for creating dye and sensitizer molecules, enabling the production of non-linear optical molecules [3-5]. Aniline represents the molecular model for aromatic amines, with its structure known in the gas phase by microwave spectroscopy and in the solid state by X-ray crystallography [6-9]. The structural and electronic properties of aniline were analyzed through semiempirical and ab initio calculations [10-14]. The presence of a substituent atom in aniline changes the charge distribution in the molecule, thereby altering its structural and electronic characteristics [15]. Aniline can form three isomeric configurations: ortho, meta, and para isomers. Ortho and para isomers have been studied theoretically and experimentally as a substitute for different atoms in the literature [16-21]. However, information on the structural and electrical properties of substitute anilines, specifically MFA (MFA) and MIA (MIA) compounds, is scarce. Therefore, future experimental research will greatly benefit from these findings. In this study, we use theoretical calculations to demonstrate the differences in the structural and electrical properties of substituted anilines.

2. MATERIAL AND METHODS

The conformer analysis of *MFA* and *MIA* was carried out by the Spartan 08 package program [22] using Merck molecular force field (MMFF) in the molecular mechanic method. then, the ground state geometries of each isomer were optimized in the gas phase using the Coulomb-attenuating method-functional hybrid Becke three-parameter Lee–Yang–Parr exchange-correlation functional (CAM-B3LYP) and the LanL2DZ basis set with the Gaussian09 program. Also, adiabatic ionization parameters were calculated by optimizing the most stable molecular conformational geometry and the same molecular geometry as the neutrals were used to calculate the vertical ionization parameters.

3. RESULTS AND DISCUSSION
3.1 Geometrical Structure Analysis

The optimized structure along with numbering of the atoms of *MFA* and *MIA* compounds obtained from the B3LYP/LANL2DZ method is show in Fig 1. The optimized structural selected bond lengths, bond angles and dihedral angles of these compounds are presented in Table 2. The energy and dipole moments values of these compounds are also displayed in Table 1.

As indicated in table 1, *MFA* has the lowest energy value of the compounds, hence it is the most stable of these compounds. In the aniline ring, our calculations of C1-C3, C1-C4, and C6-C3 bond lengths are calculated at 1.41082 1.41412, and 1.38906 Å for *MFA*. In additionally these bond lengths for *MIA* have calculated 1.41247, 1.41164, and 1.39669 respectively. each two compounds have approximately the same values among C-C bond lengths. But, C-X (X=F, I) bond lengths for fluorine and iodine atoms attached to the aniline ring were obtained as 1.39681, and 2.12926 Å respectively. As shown in Table 2, the computed bond angles and dihedral angles values for both compounds are almost the same.
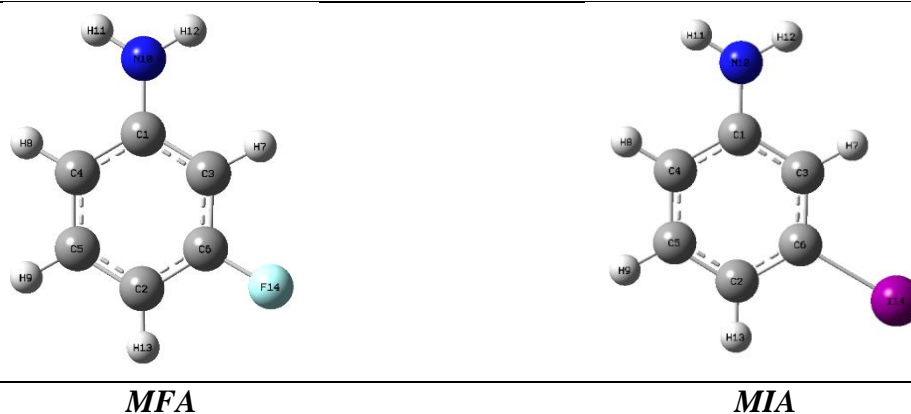

| MFA | MIA |

Figure 1. Lowest energy structure of *MFA* and *MIA* compounds

Table 1. Energy and dipole moment values of *MFA* and *MIA* compounds

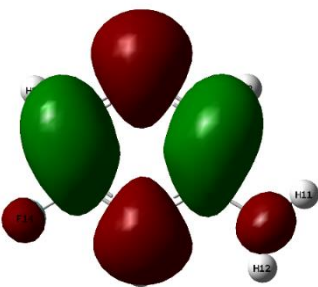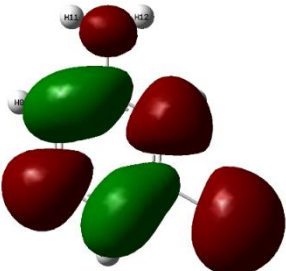| Compounds	Energy (Hartree)	Dipole Moment (Debye)	Point Group
MFA	-386.625110	3.706085	C1
MIA	-298.151130	3.244160	C1

Table 2. The Bond Lenghts (Å), Bond Angles (º) and Dihedral Angles (º) of *MFA* and *MIA* compounds

Parameters	*Compounds*

	MFA	MIA
Bond Lenghts (Å)		
N10-C1	1.38881	1.39006
C1-C3	1.41082	1.41247
C1-C4	1.41412	1.41164
C6-F14	**1.39681**	-
C6-I14	-	**2.12926**
C6-C3	1.38906	1.39669
C6-C2	1.39160	1.40004
Bond Angles (º)		
N10-C1-C3	120.38226	120.29603
N10-C1-C4	120.65442	120.71257
C1-C3-C6	118.44227	119.72753
C3-C6-F14	**117.4919**	**-**
C3-C6-I14	**-**	**118.99267**
F14-C6-C2	**118.39351**	**-**
I14-C6-C2	**-**	**119.24641**
C6-C2-C5	116.74355	118.09567
Dihedral Angles (º)		
N10-C1-C3-C6	179.99892	-179.99905
N10-C1-C4-C5	179.99113	-179.99961
F14-C6-C3-C1	**-179.98357**	**-**
I14-C6-C3-C1		**-179.99814**
F14-C6-C2-C5	**179.97602**	-
I14-C6-C2-C5	-	**179.99713**

3.2 FMO and Chemical Reactivity Descriptors

The highest occupied molecular orbital (HOMO) and the lowest unoccupied molecular orbital (LUMO) play important roles in determining the electronic, electric, and optical characteristics of molecules [23]. The LUMO functions as an electron acceptor and so describes the compounds' susceptibility to attack by nucleophiles [24]. The HOMO functions as an electron donor and so characterizes the compounds' susceptibility to assault by electrophiles. The HOMO-LUMO gap energy is the energy difference between HOMO and LUMO energies. The compositions' chemical reactivity and kinematic stability can be investigated with the help of the HOMO-LUMO gap energy. The softer the compound, the smaller the HOMO-LUMO gap energy value, and the harder, less reactive, and less stable the compound, the greater the HOMO-LUMO gap energy value [25, 26]. As seen in Figure 2, the colors red and green are represented in positive and negative phases, respectively. According to the HOMO-LUMO energy gap values, the most soft, reactive, and stable chemical is MIA.

MFA	MIA
$E_{LUMO} = -4.60 \text{ eV}$	$E_{LUMO} = -4.57 \text{ eV}$

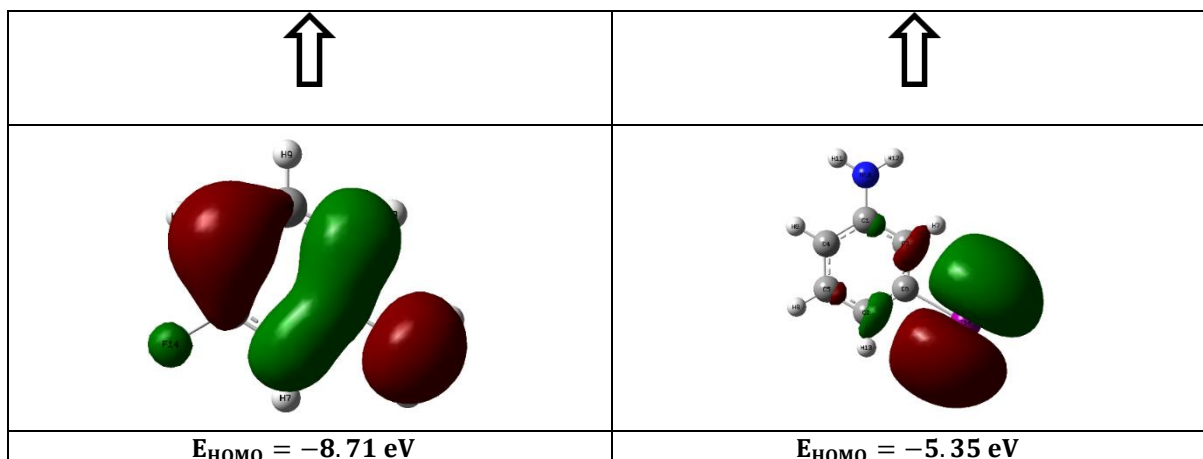| $E_{HOMO} = -8.71\ eV$ | $E_{HOMO} = -5.35\ eV$ |

Figure 2. HOMO-LUMO Plot of *MFA* and *MIA* compounds

The global chemical reactivity descriptors are defined by the Koopman's theorem [27]. the ionization potential (I) and electron affinity (A) values can be calculated through HOMO and LUMO orbitals energies using the equations $I = -E_{HOMO}$ and $A = -E_{LUMO}$. İn additionally, chemical potential (μ), global hardness (η), global softness (S), electrophilicity index (ω) and the electronegativity (χ) are expressed by the following equations. . These quantum chemical parameters were calculated using equation 1-5 [28]. The hardness corresponds to the gap between E_{HOMO} and $E_{HOMO}\ E_{LUMO}$energies and is indicator the stability and reactivity of compounds. The softness describes the capacity of an atom or a group of atoms to accept electrons. The obtainde values of global reactivity descriptors were presented in table 3

$$\mu = -\frac{(I+A)}{2}$$ Equation 1

$$\eta = \frac{(I-A)}{2}$$ Equation 2

$$S = \frac{1}{\eta}$$ Equation 3

$$\omega = \frac{\mu^2}{2\eta}$$ Equation 4

$$\chi = \frac{(I+A)}{2}$$ Equation 5

Table 3. Chemical reactivity descriptors of *MFA* and *MIA* compounds

Compounds	E_{gap} (eV)	I (eV)	A (eV)	μ (eV)	η (eV)	S (eV)	ω (eV)	χ (eV)
MFA	4.11	8.71	4.60	-6.65	2.05	0.24	10.78	6.65
MIA	0.78	5.35	4.57	-4.96	0.39	1.28	31.54	4.96

3.3 Nonlinear Optical (NLO) Properties

Nonlinear Optical (NLO) Properties is most important properties for optical modulation, optical switching, optical logic, and optical memory in the areas of telecommunications, optical interconnections, and signal processing [29-31]. The dipole moments (μ), the polarizabilities (α), and the first-order hyperpolarizabilities (β) of compounds have calculated using the finite-field approach. The obtained values were presented in table 4. The μ, (α), and β values using the x, y, z components are calculated using follows equations.

$$\mu_{tot} = \left(\mu_x + \mu_y + \mu_z\right)^{1/2}$$ Equation 6

$$\alpha_{tot} = \frac{1}{3}\left(\alpha_{xx} + \alpha_{yy} + \alpha_{zz}\right)$$ Equation 7

$$\beta_{tot} = \left(\beta_x^2 + \beta_y^2 + \beta_z^2\right)^{1/2}$$ Equation 8

were β_x, β_y and β_z are defined to be

$$\beta_x = \left(\beta_{xxx} + \beta_{xyy} + \beta_{xzz}\right) \qquad \text{Equation 9}$$
$$\beta_y = \left(\beta_{yyy} + \beta_{yzz} + \beta_{yxx}\right) \qquad \text{Equation 10}$$
$$\beta_z = \left(\beta_{zzz} + \beta_{zxx} + \beta_{zyy}\right) \qquad \text{Equation 11}$$

Total first hyper polarizability from Gaussian 09 output is given in Equation 12.

$$\beta_{tot} = \left[\left(\beta_{xxx} + \beta_{xyy} + \beta_{xzz}\right)^2 + \left(\beta_{yyy} + \beta_{yzz} + \beta_{yxx}\right)^2 + \left(\beta_{zzz} + \beta_{zxx} + \beta_{zyy}\right)^2\right]^{1/2} \quad \text{Equation 12}$$

The dipole moment is one of the most important results for electronic properties due to the distribution of charges on atoms in a compound and used to study the intermolecular interactions. The intermolecular interactions are stronger when the dipole moment is higher. A molecule's reaction to an applied electric field is characterized by its polarizability and first hyper polarizability. The calculated β_{tot} and α_{tot} values in table 4 were converted into electrostatic units (esu) (1 a.u. = 8.6393×10^{-33} esu) and (1 a.u. = 0.1482×10^{-24} esu), respectively [27, 28]. For MFA and MIA molecules, the computed dipole moment is 3.7061 D and 3.2442 D, respectively. As a result, MFA has a greater estimated dipole moment than MIA. Polarizability values for MFA and MIA compounds were determined to be 9.584 $x10^{-24}$ esu and 12.505 x 10^{-24} esu respectively. Also, both the MFA and MIA compounds' first-order hyperpolarizabilities were calculated to be 2369.14 x 10^{-33} esu and 2465.26 x 10^{-33} esu respectively. Urea is one of the model molecules used to investigate the NLO properties of compounds {Dixon, 1994 #42}. It is frequently used as a benchmark for comparison. Polarizability and first-order hyperpolarizabilities values for urea are found to be 3.8312 $x10^{-24}$esu and $0.1947 \times$ x 10^{-30} esu, respectively. Polarizability values for MFA and MIA molecules are roughly 2.5 and 3 times larger than urea, respectively. Furthermore, the first-order hyperpolarizabilities found for MFA and MIA compounds are roughly 12 and 12, 5 times larger than the magnitude of urea, respectively.

Table 4. NLO values of **MFA** and **MIA** compounds

Parameters	MFA	MIA
Dipole moment (Debye)		
μ_x	3.6862	3.0614
μ_y	0.3834	-1.0735
μ_z	0.0003	0.0000
μ_{tot}	3.7061	3.2442
Polarizability (a.u)		
α_{xx}	88.08	134.61
α_{yy}	76.82	87.98
α_{zz}	29.10	30.54
α_{tot} **(a.u)**	64.673	84.380
α_{tot} **(esu)**	9.584 $x10^{-24}$	12.505 x 10^{-24}
Hyperpolarizability (a.u)		
β_{xxx}	-153.81	45.21
β_{xxy}	196.46	139.04
β_{xyy}	-24.19	-139.23
β_{yyy}	1.34	127.60
β_{xxz}	-0.041	0.0002
β_{xyz}	0.024	-0.0009

β_{yyz}	-0.0051	-0.0011
β_{xzz}	-6.032	32.24
β_{yzz}	5.490	11.93
β_{zzz}	-0.012	-0.0027
β_{tot} (a.u)	274.229	285.354
β_{tot} (esu)	2369.14 x 10^{-33}	2465.26 10^{-33}

3.4 Mulliken Populations

The Mulliken atomic charges calculations were carried out the determination of electron population of each atom in compounds. Atomic charges have an impact on a variety of molecular characteristics, including the dipole moment, electrical parameters, polarizability, and refraction [32]. It is essential to comprehend these charges. All hydrogen atoms have positive charges, as seen in figure 3. In general, the carbon atoms in the ring have positive charges, however the C6 MIA has a negative charge and the MFA has a positive charge. Each of the two compounds' nitrogen atoms carries a negative charge. İodine and fluorine substituted atoms have positive and negative charges, respectively.
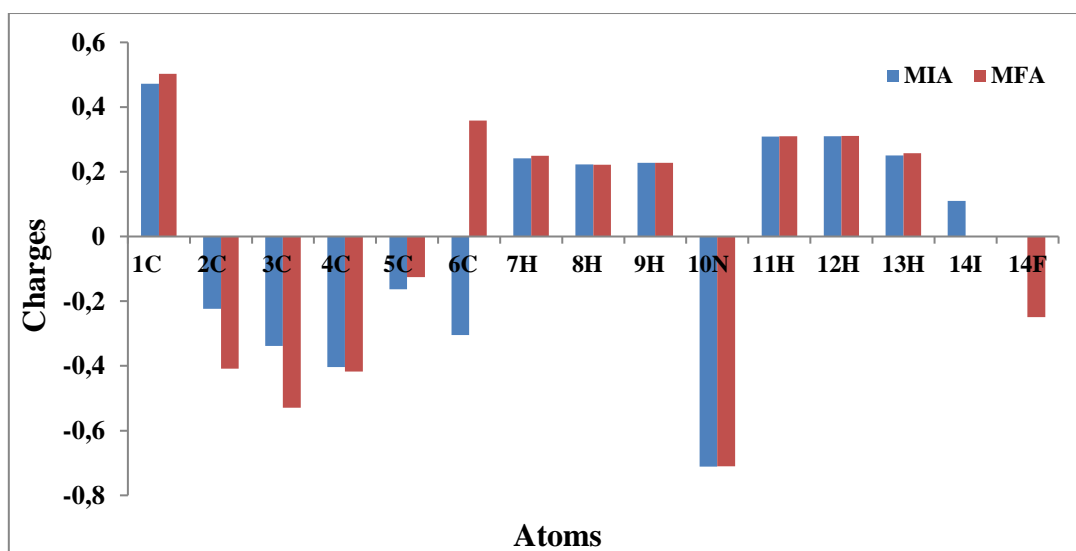

Figure 3. Mulliken populations of *MFA* and *MIA* compounds
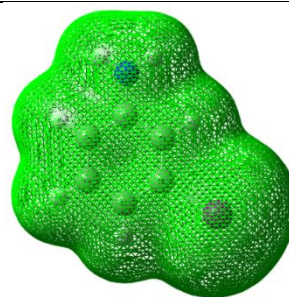
3.5 Molecular Electrostatic Potential Map

The molecular electrostatic potential maps are one of the key computation techniques used to examine the distribution of electron densities over the compounds. It is very beneficial for predicting a compound's reactivity to nucleophilic and electrophilic assaults. Intermolecular interaction types can be inferred thanks to MEPs [28, 33]. The MEP maps of the substances produced on the density surface are shown in Figure 4. These maps' red and yellow colors indicate areas that are more electron-rich (electrophilic reactivity), while their blue color indicate areas that are more electron-poor (nucleophilic reactivity). For MFA, the electrophilic and nucleophilic regions are primarily located on the fluorine atom and close to the nitrogen atom, respectively. The electrophilic region for MIA is localized on all compounds. Additionally, the color codes of these MEP maps are in the range between **-5.465×x10⁻² a.u — 5.465 ×x10⁻² a.u** and **-4.736×x10 a.u — 4.736 ×x10 a.u** MFA and MIA respectively.
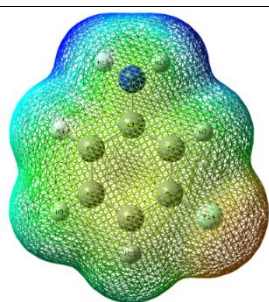
-5.465×x10^{-2} a.u — 5.465 ×x10^{-2} a.u	-4.736×x10 a.u — 4.736 ×x10 a.u
MFA	*MIA*

Figure 4. Molecular electrostatic potential of *MFA* and *MIA* compounds

3.6 Thermodynamic Properties

Table 4 shows the thermodynamic properties of MFA and MIA compounds in the gas phase, including thermal, heat capacity, entropy, zero-point vibrational energy, sum of electronic and zero-point energies, sum of electronic and thermal free energies, and rotational constants. We discovered that the heat capacity, entropy, and zero-point vibrational energy were acquired in the sequence MIA > MFA. The thermal, sum of electronic and zero-point energies, and sum of electronic and thermal free energies have been calculated in the following order: MFA > MIA. These findings can be used to conduct experiments on the chemical reactions of MFA and MIA [34]

Table 4. Thermodynamic properties for *MFA* and *MIA* compounds

Parameters	*MFA*	*MIA*
Total energy (thermal), E total (kcal. Mol^{-1})		
TOTAL	73.758	72.841
Electronic	0.000	0.000
Translational	0.889	0.889
Rotational	0.889	0.889
Vibrational	71.980	71.064
Heat capacity at const. volume, C v (cal. Mol^{-1} K^{-1})		
TOTAL	25.886	27.346
Electronic	0.000	0.000
Translational	2.981	2.981
Rotational	2.981	2.981
Vibrational	19.925	21.384
Entropy, S (cal. Mol^{-1} K^{-1})		
TOTAL	79.837	87.365
Electronic	0.000	0.000
Translational	40.030	42.054
Rotational	28.126	30.281
Vibrational	11.680	15.030
Zero-point vibrational energy, E 0 (kcal mol^{-1})	69.65156	68.27284
Sum of electronic and zero-point energies (Hartree/Particle)	-386.514113	-298.042330
Sum of electronic and thermal free energies (Hartree/Particle)	-386.507570	-298.035050
Rotational constants (GHz)		
A	3.30655	3.23079
B	1.75968	0.56568
C	1.18983	0.48139

3.7 TD-DFT Results: UV-Vis Spectra and Ionization Energies

Figure 5 depicts the calculated UV-Vis spectra of the neutral m-fluoroaniline and m-iodoaniline isomers using time-dependent density functional theory (TD-DFT). The spectra demonstrate strong absorption bands at around 190 nm and weaker absorption bands at around 210 nm. The major contributions to the electronic transitions of the m-fluoroaniline and m-iodoaniline isomers are presented in Tables 6 and 7, respectively. Specifically, the first excited state of the m-fluoroaniline isomer arises from the transition of the highest occupied molecular orbital (HOMO) to the lowest unoccupied molecular orbital (LUMO), while the most intense transition in the m-iodoaniline isomer results from the combined transitions of H-1 to LUMO and H-1 to L+1. These findings offer valuable insights into the electronic structure and bonding of the isomers and can facilitate the interpretation of their spectroscopic properties.
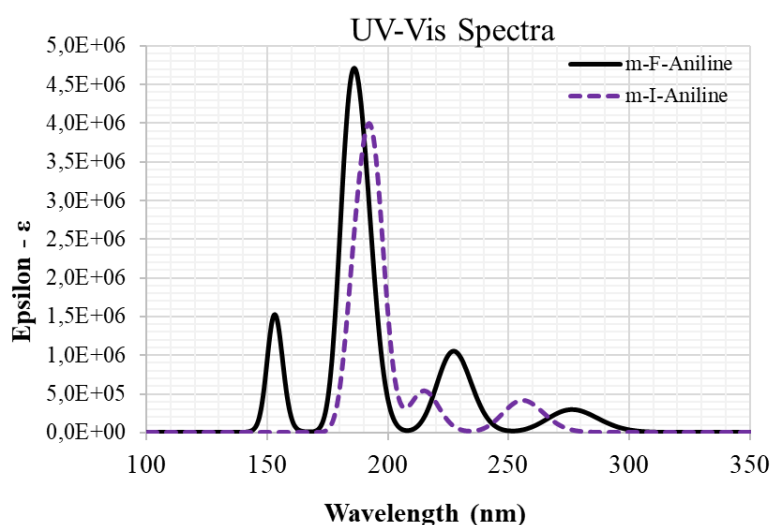

Figure 5. Calculated UV-Vis spectra of the titled molecules (GaussSum program was used to plot spectra)

The Table 5. shows the energy values and dipole moments for different isomers of m-fluoroaniline and m-iodoaniline. For m-fluoroaniline, there are slight differences in the relative energy values between the Adiabatic Ionization (AI) and Vertical Ionization (VI) processes, indicating that the VI process requires more energy to ionize the molecule. For m-iodoaniline, there is only an AI process, and the relative energy values are consistent across different units. The dipole moment values for the isomers indicate that m-iodoaniline is more polar than m-fluoroaniline. These numerical values can provide valuable information about the properties and behavior of these molecules.

Table 5. Molecular energies (relative to its neutrals) and dipole moments of the molecules (AI: Adiabatic Ionization, VI: Vertical Ionization)

Isomers	Energy (Hartree)	Relative Energy (Hartree)	Relative Energy (kcal/mol)	Relative Energy (cm^{-1})	Relative Energy (eV)	Dipole Moment (D)
m-fluoroaniline (AI)	-386,337	0,288	756,115	180,716	7,837	6,370
m-fluoroaniline (VI)	-386,332	0,293	184,066	64376,696	7,982	6,555
m-iodoaniline (AI)	-297,866	0,286	179,217	62680,632	7,772	10,953
m-iodoaniline (VI)	-297,866	0,286	179,217	62680,632	7,772	10,953

The Table 6. shows that the first excited state (State 1) corresponds to a transition from HOMO to LUMO, which accounts for 79% of the transition. State 2 corresponds to a transition from HOMO to L+1, which accounts for 86% of the transition. The contributions of HOMO to L+2 and L+3 are the major contributors to State 3, with a total percentage of 97%. State 4 involves a combination of transitions from H-1 to LUMO and HOMO to L+2, accounting for 79% of the transition. State 5 corresponds to a transition from HOMO to L+4, which accounts for 87% of the transition.

States 6, 8, and 7 correspond to transitions from H-1 to LUMO and H-1 to L+1, HOMO to L+5 and L+6, and HOMO to L+5 and L+6, respectively, with different percentages of contribution. State 9 involves transitions from H-1 to L+2 and L+3, accounting for 83% of the transition, while State 10 involves transitions from H-1 to L, H-1 to L+2, and H to L+2 with different contributions. Overall, the table provides valuable information on the excited states and electronic transitions of the m-fluoroaniline isomer.

Table 6. TD-DFT results for the excited states of the neutral m-fluoroaniline isomer (f is the oscillator strength)

Excited State	ΔE (nm)	f	Major Contributions to the Transitions (percentage)
1	261.603141774	0.0003	HOMO→LUMO (79%)
2	255.737697267	0.0671	HOMO→L+1 (86%)
3	243.421276578	0.0001	HOMO→L+2 (11%), HOMO→L+3 (86%)
4	228.138580599	0.0005	H-1→LUMO (18%), HOMO→L+2 (61%)
5	214.903355714	0.0871	HOMO→L+4 (87%)
6	193.664781337	0.538	H-1→LUMO (14%), H-1→L+1 (75%)
7	187.658649309	0.0003	HOMO→L+5 (69%), HOMO→L+6 (21%)
8	186.532155341	0.2944	HOMO→L+5 (24%), HOMO→L+6 (71%)
9	184.272688513	0.0001	H-1→L+2 (10%), H-1→L+3 (83%)
10	168.761747468	0.0	H-1→L (31%), H-1→L+2 (22%), H→L+2 (12%)

The major contributions to the transitions are identified by the orbitals involved in the transitions. H-1 and L+1 represent the highest occupied molecular orbital (HOMO) and lowest unoccupied molecular orbital (LUMO), respectively, while L+2, L+3, and L+4 represent the second, third, and fourth lowest unoccupied molecular orbitals, respectively.

The Table 7. shows that the most intense transition occurs at a wavelength of 179.46 nm with an oscillator strength of 0.3649 and is dominated by the H-1 to LUMO transition (45%) and H-1 to L+1 transition (31%). Additionally, the table shows that the contributions of higher energy transitions (such as those involving L+2, L+3, and L+4) are relatively small.

Table 7. TD-DFT results for the excited states of the neutral m-iodoaniline isomer (f is the oscillator strength)

Excited State	ΔE (nm)	f	Major Contributions to the Transitions (percentage)
1	247.211917557	0.048	H-1->L+1 (14%), HOMO->LUMO (83%)
2	209.397387286	0.1709	H-1->LUMO (16%), HOMO->L+1 (80%)
3	179.458361817	0.3649	H-1->LUMO (45%), H-1->L+1 (31%), HOMO->L+1 (12%)
4	174.21095282	0.57	H-1->LUMO (35%), H-1->L+1 (48%)
5	167.993432533	0.0	HOMO->L+2 (95%)
6	156.965859387	0.0014	HOMO->L+3 (94%)

7	147.7920075	0.2448	H-2->LUMO (91%)
8	145.709475863	0.0028	HOMO->L+4 (71%)
9	144.97683935	0.0014	H-3->LUMO (86%)
10	141.761025626	0.0031	H-1->L+3 (78%), HOMO->L+4 (11%)

These results provide valuable information about the electronic properties and behavior of the m-iodoaniline isomer, which can be useful for understanding its reactivity and potential applications in various fields.

4. CONCLUSION

In this study, we performed detailed investigations on MFA and MIA molecules using quantum chemical calculations. The structural, electronic, and UV-Vis analyses of the title compounds were calculated by the DFT/CAMB3LYP/LanL2DZ method. Our results show that substituents attached to the benzene ring of aniline produce both structural and electronic distortions, with the HOMO-LUMO gap values being one of the most significant effects. Additionally, the polarizability values for MFA and MIA molecules are roughly 2.5 and 3 times larger than urea, respectively. The first order hyperpolarizabilities found for MFA and MIA compounds are roughly 12 and 12.5 times larger than the magnitude of urea, respectively. According to Mulliken population analysis, all hydrogen atoms have positive charges, while the carbon atoms in the ring generally have positive charges. However, C6 MIA has a negative charge, and MFA has a positive charge. In summary, the UV-Vis spectra of the m-fluoroaniline and m-iodoaniline isomers were calculated using TD-DFT, with strong absorption bands observed at around 190 nm and weaker absorption bands at around 210 nm. The major electronic transitions and excited states of the isomers were identified, providing insights into their electronic structure and bonding. Additionally, energy values and dipole moments were determined for the isomers, offering further information about their properties and behavior. These findings can be useful for interpreting the spectroscopic properties of the isomers and understanding their potential applications in various fields.

References

1. Nalwa, H.S., *Handbook of organic conductive molecules and polymers*. 1997: Wiley.
2. Vaschetto, M.E., B.A. Retamal, and A.P.J.J.o.M.S.T. Monkman, *Density functional studies of aniline and substituted anilines*. 1999. **468**(3): p. 209-221.
3. Agbor, N., et al., *An optical gas sensor based on polyaniline Langmuir-Blodgett films*. 1997. **41**(1-3): p. 137-141.
4. Morley, J.O.J.T.J.o.P.C., *Nonlinear optical properties of organic molecules. 19. Calculations of the structure, electronic properties, and hyperpolarizabilities of phenylsydnones*. 1995. **99**(7): p. 1923-1927.
5. Naik, P., et al., *Improvement in performance of N3 sensitized DSSCs with structurally simple aniline based organic co-sensitizers*. 2018. **174**: p. 999-1007.
6. Wang, Y., S. Saebø, and C.U.J.J.o.M.S.T. Pittman Jr, *The structure of aniline by ab initio studies*. 1993. **281**(2-3): p. 91-98.
7. Lister, D. and J.J.C.C. Tyler, *Non-planarity of the aniline molecule*. 1966(6): p. 152-153.

8.   Lister, D., et al., *The microwave spectrum, structure and dipole moment of aniline.* 1974. **23**(2): p. 253-264.

9.   Fukuyo, M., et al., *The structure of aniline at 252 K.* 1982. **38**(2): p. 640-643.

10.   Hehre, W.J., L. Radom, and J.A.J.J.o.t.A.C.S. Pople, *Molecular orbital theory of the electronic structure of organic compounds. XII. Conformations, stabilities, and charge distributions in monosubstituted benzenes.* 1972. **94**(5): p. 1496-1504.

11.   Parr, W.J. and R.E.J.J.o.M.S. Wasyushen, *A MINDO/3 study of the planarity of the amino-fragment in some para-substituted anilines.* 1977. **38**: p. 272-276.

12.   Gorse, A.-D. and M.J.J.o.M.S.T. Pesquer, *A theoretical study of aniline and some derivatives in their ground states.* 1993. **281**(1): p. 21-32.

13.   Moghaddam, F.M., R. Pourkaveh, and A.J.T.J.o.O.C. Karimi, *Oxidative heck reaction as a tool for para-selective olefination of aniline: a DFT supported mechanism.* 2017. **82**(19): p. 10635-10640.

14.   Kurt, M., M. Yurdakul, and Ş.J.J.o.M.S.T. Yurdakul, *Molecular structure and vibrational spectra of 3-chloro-4-methyl aniline by density functional theory and ab initio Hartree-Fock calculations.* 2004. **711**(1-3): p. 25-32.

15.   Vaschetto, M.E. and B.A.J.T.J.o.P.C.A. Retamal, *Substituents effect on the electronic properties of aniline and oligoanilines.* 1997. **101**(37): p. 6945-6950.

16.   Errabelli, R., Z. Zheng, and A.B.J.J.o.t.A.S.f.M.S. Attygalle, *Formation of Protonated ortho-Quinonimide from ortho-Iodoaniline in the Gas Phase by a Molecular-oxygen-mediated, ortho-Isomer-specific Fragmentation Mechanism.* 2020. **31**(4): p. 864-872.

17.   Hand, R.L. and R.F.J.J.o.t.E.S. Nelson, *The Anodic Decomposition Pathways of Ortho-and Meta-substituted Anilines.* 1978. **125**(7): p. 1059.

18.   Tian, C., et al., *Visible-Light Mediated ortho-Trifluoromethylation of Aniline Derivatives.* 2019. **84**(21): p. 14241-14247.

19.   Oyama, M. and K.J.E.a. Kirihara, *Spectroscopic investigation of oxidation products of ortho- or meta-substituted aniline derivatives in acetonitrile using an electron-transfer stopped-flow method.* 2004. **49**(22-23): p. 3801-3806.

20.   Kessar, S.V., et al., *A Study of BF3-Promoted ortho Lithiation of Anilines and DFT Calculations on the Role of Fluorine–Lithium Interactions.* 2008. **120**(25): p. 4781-4784.

21.   Rahman, S., et al., *Spectroscopic and DFT studies of the charge transfer complexation of iodine with aniline and its derivatives in carbon tetrachloride medium.* 2022. **351**: p. 118667.

22.   Shao, Y., et al., *Advances in methods and algorithms in a modern quantum chemistry program package.* Physical Chemistry Chemical Physics, 2006. **8**(27): p. 3172-3191.

23.   Fleming, I., *Molecular orbitals and organic chemical reactions.* 2011: John Wiley & Sons.

24.   Karelson, M., V.S. Lobanov, and A.R.J.C.r. Katritzky, *Quantum-chemical descriptors in QSAR/QSPR studies.* 1996. **96**(3): p. 1027-1044.

25.   Sheela, N., et al., *Molecular orbital studies (hardness, chemical potential and electrophilicity), vibrational investigation and theoretical NBO analysis of 4-4'-(1H-1, 2, 4-triazol-1-yl methylene) dibenzonitrile based on abinitio and DFT methods.* 2014. **120**: p. 237-251.

26.   Miar, M., et al., *Theoretical investigations on the HOMO–LUMO gap and global reactivity descriptor studies, natural bond orbital, and nucleus-independent chemical shifts analyses of 3-phenylbenzo [d] thiazole-2 (3 H)-imine and its para-substituted derivatives: Solvent and substituent effects.* 2021. **45**(1-2): p. 147-158.

27.   Koopmans, T.J.P., *The classification of wave functions and eigen-values to the single electrons of an atom.* 1934. **1**(1): p. 104-113.

28.   Ekincioğlu, Y., H.Ş. Kılıç, and Ö.J.B.J.o.P. Dereli, *DFT Study of Conformational Analysis, Molecular Structure and Properties of para-, meta-and ortho 4-Methoxyphenyl Piperazine Isomers.* 2021. **51**(4): p. 958-968.

29.   Andraud, C., et al., *Theoretical and experimental investigations of the nonlinear optical properties of vanillin, polyenovanillin, and bisvanillin derivatives.* 1994. **116**(5): p. 2094-2102.

30. Wu, J., J. Luo, and A.K.-Y.J.J.o.M.C.C. Jen, *High-performance organic second-and third-order nonlinear optical materials for ultrafast information processing.* 2020. **8**(43): p. 15009-15026.

31. Suresh, S. and D.J.R.A.M.S. Arivuoli, *Nanomaterials for nonlinear optical (NLO) applications: a review.* 2012. **30**(3): p. 243-253.

32. De Proft, F., et al., *Atomic charges, dipole moments, and Fukui functions using the Hirshfeld partitioning of the electron density.* 2002. **23**(12): p. 1198-1209.

33. Sjoberg, P. and P.J.J.o.P.C. Politzer, *Use of the electrostatic potential at the molecular surface to interpret and predict nucleophilic processes.* 1990. **94**(10): p. 3959-3961.

34. Lillo-Ródenas, M., D. Cazorla-Amorós, and A.J.C. Linares-Solano, *Understanding chemical reactions between carbons and NaOH and KOH: an insight into the chemical activation mechanism.* 2003. **41**(2): p. 267-275.